

# A New Selective Technique for Characterization of Polycyclic Aromatic Hydrocarbons in Complex Samples: UV Resonance Raman Spectrometry of Coal Liquids

*Sir:* We recently demonstrated (1) that UV resonance Raman spectroscopy (UVRRS) could detect polycyclic aromatic hydrocarbons (PAH's) such as naphthalene, anthracene, and pyrene down to the 20 ppb level in solvents such as water and acetonitrile. The Raman spectra could be used to speciate between derivatives as similar as 2-methyl- and 9-methyl-anthracene. More recently we proposed (2) that little interference from fluorescence occurs for UV Raman measurements below 250 nm; few compounds which have their first excited singlet states below 250 nm have significant fluorescence quantum yields.

The earlier results (1) on pure compounds suggested that UVRRS could be useful for studying PAH's in complex matrices and suggested that UVRRS could be superior in some instances to fluorescence detection; the room temperature Raman spectra show numerous narrow bands which can be used for speciation. In contrast, room-temperature PAH fluorescence spectra are often broad and featureless. We also suggested that UV Raman intensities may be a more reliable measure of PAH concentration in complex matrices than fluorescence intensities. The UV Raman intensities are less susceptible to collisional quenching because the UV Raman excitations used in our studies occur in the second or third excited PAH singlet states which have short (subpicosecond) lifetimes due to fast internal conversion rates.

We wish to report evidence that UV resonance Raman spectroscopy (UVRRS) is a powerful technique for the identification and quantitation of polycyclic aromatic hydrocarbons (PAH's) in a coal liquid. Our results suggest that this technique will be of general utility for the study of systems containing chromaphoric species absorbing in the UV spectral region. In this paper we demonstrate that (1) the resonance Raman spectra of PAH derivatives can be selectively observed in solutions of coal liquids and (2) different UV excitation wavelengths result in the selective Raman enhancement of different polycyclic aromatic hydrocarbon ring systems.

## EXPERIMENTAL SECTION

The coal liquid sample was prepared by the direct hydrogenation of coal and is a heavy distillate recovered between 340 and 510 °C. Acetonitrile was obtained as a high-purity UV grade solvent from Burdick and Jackson. The PAH derivatives were obtained from Chem Services, West Chester, PA, and the Raman spectra were measured with a tunable UV Raman spectrometer described in detail elsewhere (3). The excitation source was a frequency doubled Nd-YAG laser which pumped a dye laser which was subsequently frequency doubled. The dye laser frequency doubled light was mixed with 1.06 $\mu$  Yag fundamental to generate excitation light below 260 nm. The Raman scattered light was dispersed with a modified Spex Triplemate monochromator. A PAR OMA2 intensified Reticon array was used to detect the Raman scattered light. The detector was gated on for 10-ns intervals which bracketed the UV excitation pulse.

The coal liquid sample (dissolved in acetonitrile) was measured by flowing the solution through a lamellar jet nozzle. The jet, which was ca. 200  $\mu$ m in width and 5 mm high, was optically uniform. The laser beam was slightly defocused in the jet (to avoid nonlinear phenomena) and the scattered light was collected at 90°.

Each of the Raman spectra shown have the Raman spectrum of the solvent, acetonitrile, digitally subtracted; due to the short path length of the jet the acetonitrile spectrum did not require any correction for self-absorption prior to subtraction. To ensure that the solvent did not lead to artifacts in the 1300-1400  $\text{cm}^{-1}$

region, the coal liquid samples were also measured in methanol solution; methanol has no interfering Raman peaks in the 1350-1450  $\text{cm}^{-1}$  region.

## RESULTS AND DISCUSSION

Figure 1 shows the absorption spectrum of the coal liquid sample dissolved in acetonitrile along with the absorption spectra of a number of polycyclic aromatic hydrocarbons such as naphthalene, fluorene, anthracene, phenanthrene, triphenylene, and pyrene; the broad absorption spectrum of the coal liquid sample derives from the overlap of the absorption bands of numerous PAH derivatives (4). As is evident from the absorption spectra of the pure PAH components, as the size of the conjugated macrocycle increases, the  $\lambda_{\text{max}}$  of the PAH absorption spectra also increase. For example, naphthalene shows a strong absorption band at ca. 220 nm with a weaker series of bands centered at ca. 275 nm. Anthracene, phenanthrene, triphenylene, and pyrene show their absorption maxima at 251, 251, 256, and 239 nm, respectively. Pyrene shows a more complex spectrum with strong absorption bands at 239, 272, and 334 nm. The absorption spectra of all of these derivatives show shoulders and subsidiary peaks on the short wavelength side of each of the strong absorption bands. These subsidiary peaks derive from vibronic Franck-Condon absorption components.

A comparison between the absorption spectrum of the coal liquid sample with that of the pure PAH components suggests that pyrene derivatives would contribute to the small coal liquid absorption peak centered to 335 nm, while derivatives of triphenylene, phenanthrene, anthracene, and fluorene would contribute to the broad coal liquid band at 255 nm. Naphthalene and fluorene derivatives would contribute to the coal liquid absorption spectrum between 200 and 220 nm. This tabulation must, of course, be incomplete since these components represent only a small fraction of the PAH species present in the coal liquid sample (4).

Since the cross section for resonance Raman scattering from these compounds is expected to increase nonlinearly with the molar absorptivity of the resonant species, excitation at the  $\lambda_{\text{max}}$  of a pure PAH component should selectively enhance the Raman spectrum of that species by an amount proportional to its relative concentration and its resonant Raman cross section.

Figure 2 shows a series of resonance Raman spectra of the coal liquid sample diluted by ca. 1000 in acetonitrile. The acetonitrile Raman peaks at 918 and 1376  $\text{cm}^{-1}$  have been numerically subtracted from each of the spectra. The Raman spectrum of the coal liquid sample excited at 256 nm shows as its major feature a broad peak with a maximum at 1624  $\text{cm}^{-1}$  with shoulders at 1600 and 1577  $\text{cm}^{-1}$ . A weaker broad feature at ca. 1400  $\text{cm}^{-1}$  shows a shoulder at 1340  $\text{cm}^{-1}$  and other features at 1355, 1409, 1436, and 1479  $\text{cm}^{-1}$ . Other peaks occur at 757, 824, and 1035  $\text{cm}^{-1}$ .

The spectrum excited at 235 nm in Figure 2b is dramatically different. The major feature is a peak at 1380  $\text{cm}^{-1}$  with a shoulder at 1420  $\text{cm}^{-1}$ . The peak at 1628  $\text{cm}^{-1}$  now shows a shoulder at 1587  $\text{cm}^{-1}$ . Also peaks occur at 718, 757, 1068, 1185, and 1239  $\text{cm}^{-1}$ .

Excitation at 230 nm (Figure 2c) results in a strong peak at 1376  $\text{cm}^{-1}$ , a shoulder at 1420  $\text{cm}^{-1}$ , and new features at 1463 and 1531  $\text{cm}^{-1}$ . A doublet appears at 1589 and 1611  $\text{cm}^{-1}$ . The high frequency peak which was centered at ca. 1610  $\text{cm}^{-1}$  for

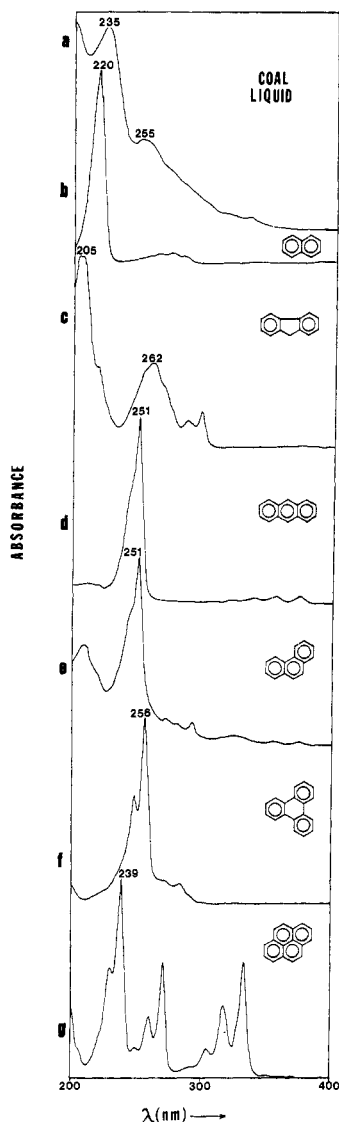


**Figure 1.** Absorption spectra of polycyclic aromatic hydrocarbons in  $\text{CH}_3\text{CN}$  (path length = 1 cm): (a) coal liquid sample; (b) naphthalene; (c) fluorene; (d) anthracene; (e) phenanthrene; (f) triphenylene; (g) pyrene.

256-nm excitation has shifted to ca.  $1600\text{ cm}^{-1}$  with 230-nm excitation. Other features observed with 230-nm excitation include peaks at 760, 1187, and  $1230\text{ cm}^{-1}$ .

Excitation at 220 nm shows two broad features centered at  $1376$  and  $1592\text{ cm}^{-1}$  with shoulders at 1461, 1532, and  $1649\text{ cm}^{-1}$ . The breadth of the peaks mainly results from the decrease in the spectral resolution for the spectrum excited at 220 nm; for a given spectrometer slit setting the spectral energy resolution ( $\text{cm}^{-1}$ ) depends upon the reciprocal of the wavelength.

A comparison between the coal liquid resonance Raman spectra and the resonance Raman spectra of pure PAH derivatives illustrates the contribution of different PAH ring systems to the resonance Raman spectra of the coal liquid sample. For example, Figure 3 shows the resonance Raman spectra of anthracene, phenanthrene, triphenylene, pyrene, fluorene, and naphthalene. In addition, naphthalene Raman spectra are shown for excitation at 255, 235, and 220 nm. With excitation at 255 nm, anthracene and phenanthrene show intense Raman peaks at  $1400$  and  $1398\text{ cm}^{-1}$ , respectively, while triphenylene shows a strong peak at ca.  $1337\text{ cm}^{-1}$ . Thus, the shoulder at ca.  $1340\text{ cm}^{-1}$  in the coal liquid sample excited at 255 nm may derive from a triphenylene derivative, while the higher frequency components at ca.  $1400\text{ cm}^{-1}$  may derive

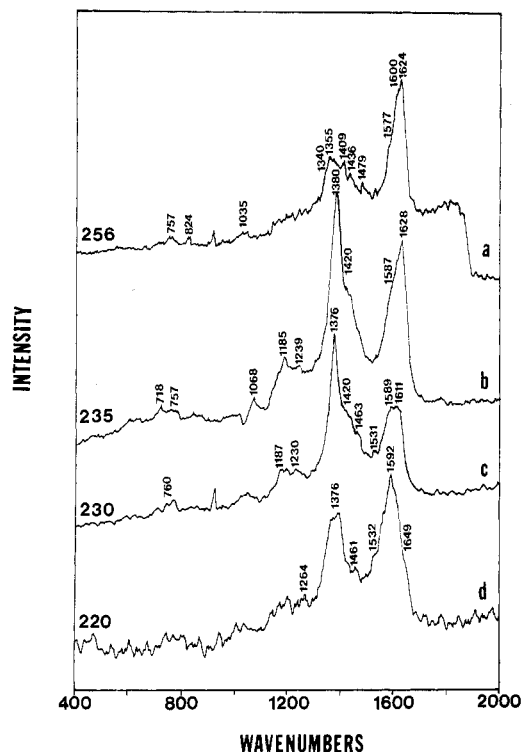


**Figure 2.** Resonance Raman spectra of a coal liquid sample dissolved in  $\text{CH}_3\text{CN}$ : (a)  $\lambda_{\text{ex}} = 256\text{ nm}$ , average power, 2.0 mW; number of pulses averaged, 18 000 (i.e., 15 min scan); spectrometer band-pass, ca.  $6.0\text{ cm}^{-1}$ ; (b)  $\lambda_{\text{ex}} = 235\text{ nm}$ ; average power, 15.0 mW; number of pulses averaged, 30 000; spectrometer band-pass ca.  $13\text{ cm}^{-1}$ ; (c)  $\lambda_{\text{ex}} = 230\text{ nm}$ ; average power, 5.0 mW; number of pulses averaged, 18 000; spectrometer band-pass, ca.  $13\text{ cm}^{-1}$ ; (d)  $\lambda_{\text{ex}} = 220\text{ nm}$ ; average power, 12 mW; number of pulses averaged, 36 000; spectrometer band-pass, ca.  $58\text{ cm}^{-1}$ . Note that the  $\text{CH}_3\text{CN}$  spectral features have been numerically subtracted in the spectra shown.

from fused ring systems containing three rings such as anthracene and phenanthrene. The strong peak centered at ca.  $1610\text{ cm}^{-1}$  in the 255-nm excited coal liquid spectrum may have contributions from ring systems based on pyrene ( $1624\text{ cm}^{-1}$ ), fluorene ( $1611\text{ cm}^{-1}$ ), and naphthalene ( $1629\text{ cm}^{-1}$ ). The peaks at 760, ca. 1030, 1230, and ca.  $1260\text{ cm}^{-1}$  in the coal liquid samples also show counterparts in the resonance Raman spectra of the pure PAH derivatives.

As the Raman excitation wavelength is changed, alterations occur in the relative intensities of the Raman peaks of the pure PAH derivatives. For example, the  $1611\text{ cm}^{-1}$  peak dominates the resonance Raman spectrum of naphthalene with 255-nm excitation. In contrast, for 235-nm excitation the  $1374\text{ cm}^{-1}$  naphthalene peak is the most intense feature, while for 220-nm excitation the  $1374\text{ cm}^{-1}$  peak dominates the spectrum. Thus, the increase in intensity of the coal liquid Raman peak at ca.  $1380\text{ cm}^{-1}$  between the spectra excited at 256 and 235 nm probably derives from naphthalene derivatives.

A decreased contribution for the  $1624\text{ cm}^{-1}$  peak of pyrene in the coal liquid Raman spectrum as the excitation wavelength is decreased to 220 nm probably accounts for the shift for the ca.  $1610\text{ cm}^{-1}$  coal liquid peak to lower frequency; as the excitation wavelength is shifted off of the pyrene absorption spectral maximum, a decrease will occur in the pyrene resonance Raman intensities.

The correlations discussed above between the resonance Raman spectra and that from the coal liquid sample are at best qualitative. Similar coal liquid samples which were previously characterized by GC, LC, and MS have contained a myriad of different hydrocarbon and heterocyclic fused ring systems with almost every possible hydrocarbon and heteroatom substitution pattern (4). Since we have as yet only

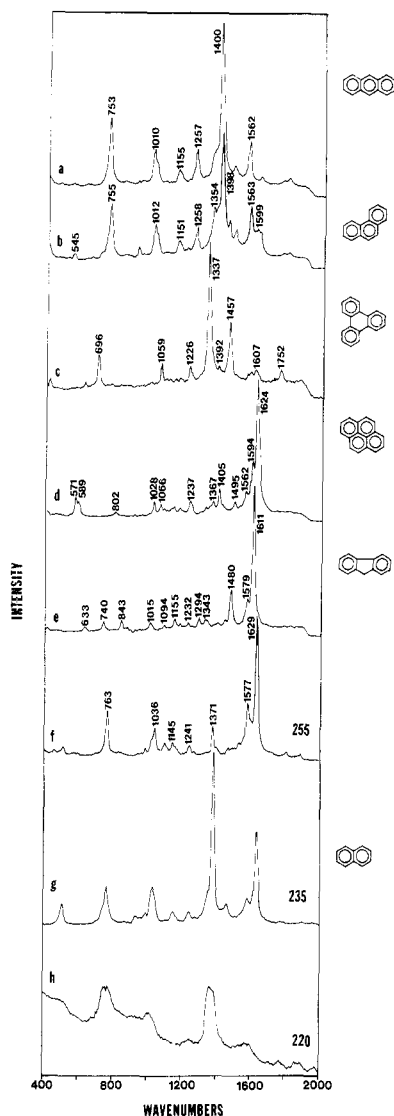


**Figure 3.** Resonance Raman spectra of  $5 \times 10^{-3}$  M solutions of PAH derivatives dissolved in acetonitrile: (a) anthracene; (b) phenanthrene; (c) triphenylene; (d) pyrene; (e) fluorene; (f) naphthalene; (g) naphthalene ( $\lambda_{\text{ex}} = 235$  nm; average power, 5.0 mW; number of pulses averaged, 18 000; spectrometer band-pass, ca.  $13 \text{ cm}^{-1}$ ); (h) naphthalene ( $\lambda_{\text{ex}} = 220$  nm; average power, 12.0 mW; number of pulses averaged, 12 000; spectrometer band-pass, ca.  $15 \text{ cm}^{-1}$ ). The peaks from the solvent have been numerically subtracted. Experimental conditions for spectra a–f are as follows:  $\lambda_{\text{ex}} = 255$  nm; average power, 2.5 mW; number of pulses average, 36 000 (i.e., 30 min scan); spectrometer band-pass ca.  $12 \text{ cm}^{-1}$ .

measured the UV resonance Raman spectra of a small number of PAH derivatives, it is not yet possible to uniquely identify or quantitate individual PAH species in the coal liquid sample. However, the correlations between spectral features in the coal liquid sample and PAH ring systems are probably qualitatively reliable since the Raman spectrum of a substituted PAH will closely resemble that of the parent ring system. The resonance Raman enhanced peaks derive from vibrations of the fused ring systems. As noted from studies of phenyl- and methyl-substituted anthracenes (1), ring substitution results in small frequency shifts and changes in relative intensities. No new peaks appear which are due to vibrations of ring substituents or from vibrations between the substituent and the fused ring. Resonance Raman enhancement only occurs if the nuclear displacements in a vibration are active in the electronic transition. Thus, unless the orbitals involved in the electronic transition significantly extend into the substituent, little enhancement for substituent vibrations is expected; the phenyl group substituent in anthracene does not result in an increase

in the conjugation of the  $\pi$  orbitals of the anthracene ring into the phenyl group, and thus no phenyl vibrations are resonant enhanced.

The results above indicate that while specific PAH ring systems can be selectively observed with different excitation wavelengths, the ring substituent patterns cannot, as yet, be unambiguously determined with the data available. However, the results above clearly indicate that classes of PAH's are selectively enhanced with particular excitation wavelengths in the UV spectral regions. For example, the data indicate naphthalene derivatives are most enhanced with excitation at shorter wavelengths while the larger ring systems such as pyrene, anthracene, and triphenylene are enhanced with longer excitation wavelengths.

For any excitation wavelength the intensities of the Raman peaks relative to that of the solvent are directly proportional to the PAH concentration (1). Thus, if an isolated Raman peak were present for one PAH analyte in a coal liquid sample, and the Raman excitation profile were known for that analyte relative to some solvent standard, the PAH concentration in the coal liquid sample could be calculated from the relative intensity of the PAH Raman peak. Indeed, the excitation profiles would be a rich source of data because numerous maxima will occur at the individual vibronic components of each absorption band.

We are investigating techniques to increase the selectivity of UVRRS. Selectivity in UV resonance Raman spectroscopy derives from two sources, the number of resolved Raman peaks present and the magnitude of the selective enhancement shown by one species at a particular excitation wavelength compared to that of the remaining species in the mixture. We expect that low-temperature measurements will result in a dramatic increase in selectivity; low temperature IR matrix isolation spectral measurements (5) show  $1 \text{ cm}^{-1}$  vibrational peak widths for PAH's in contrast to the ca.  $15 \text{ cm}^{-1}$  widths we observe for our room temperature measurements. An increase in selectivity would also derive from narrowing of the Raman excitation profiles. Shpol'skii and matrix isolation, as well as more conventional low temperature absorption, fluorescence, and phosphorescence spectroscopic studies of PAH's demonstrate dramatic line narrowing of the absorption and emission bands as the sample temperature is lowered (5, 6). Excitation at the narrow low-temperature absorption band maxima would result in a true resonance with more of the analyte molecules in the sample if inhomogeneous broadening dominates the spectra line width at room temperature (7). If the homogeneous line width,  $\Gamma$ , decreases, the excitation profiles will become sharper and more intense since the intensity and the excitation profile width,  $W$ , depends upon the reciprocal of the homogeneous line width,  $W = K(\Gamma)^{-n}$ , where  $K$  is a constant which depends upon the exact Raman enhancement mechanism,  $n$  is predicted to be between 2 and 4.

Fluorescence has not significantly interfered with any of the resonance Raman measurements of the coal liquid sample. This is due to the fact that few molecular species exist which have their first excited singlet state below 260 nm and also have significant fluorescent quantum yields in the condensed state (2). In contrast, excitation in the near-UV and visible spectral region would result in a high fluorescence intensity which would swamp any Raman spectral measurements.

## CONCLUSIONS

The data presented here indicate that UV resonance Raman spectroscopy is a new technique which, because of its selectivity and sensitivity, is uniquely capable of monitoring PAH species in complex matrices. UV resonance Raman studies of PAH species should be much less susceptible to matrix interference effects than is fluorescence spectroscopy since

the quenching phenomena which lead to interference in fluorescence spectroscopy will not affect the Raman intensities. Extension of this work to low temperature should result in even higher selectivities and sensitivities. It is likely that UV resonance Raman spectroscopy will become a powerful new technique for characterizing complex samples containing chromophores absorbing in the UV spectral region.

#### ACKNOWLEDGMENT

We gratefully acknowledge Gerst Gibbon, Curt White, and Bernard Blaustein from the Pittsburgh Energy Technology Center, U.S. Department of Energy, for the gift of the coal liquid sample and for helpful discussions.

#### LITERATURE CITED

- (1) Asher, S. A. *Anal. Chem.* **1984**, *56*, 720.
- (2) Asher, S. A.; Johnson, C. R. *Science* **1984**, *225*, 311.
- (3) Asher, S. A.; Johnson, C. R.; Murtaugh, J. *Rev. Sci. Instrum.* **1983**, *54*, 1657.

- (4) White, C. M. "Handbook of Polycyclic Aromatic Hydrocarbons"; Bjorseth, A., Ed.; Marcel Dekker: New York, 1983; p 525.
- (5) Wehry, E. L. "Handbook of Polycyclic Aromatic Hydrocarbons"; Bjorseth, A., Ed.; Marcel Dekker: New York, 1983; p 323.
- (6) Lee, M. L.; Novotny, M. V.; Barite, K. D. "Analytical Chemistry of Polycyclic Aromatic Compounds"; Academic Press: New York, 1981; p 290.
- (7) Long, D. A. "Raman Spectroscopy"; McGraw-Hill: New York, 1977.

Craig R. Johnson  
Sanford A. Asher\*

Department of Chemistry  
University of Pittsburgh  
Pittsburgh, Pennsylvania 15260

RECEIVED for review April 4, 1984. Accepted June 15, 1984. This work was supported by the U.S. Public Health Service through Grant 1R01GM30741-02 and from a Cottrell Research Corp. Grant as well as from an NSF instrumentation grant (Grant PCM-8115738).

## Use of Teflon Components in Photochemical Reactors

Sir: In recent years, several workers (1, 2) have advocated the use of Teflon reaction coils in postcolumn photochemical reaction detectors for high-performance liquid chromatography (HPLC). The major advantages of Teflon over quartz are that it is less fragile and more readily manipulated. Teflon FEP transmits UV light at wavelengths above 240 nm although the transmittance falls below 280 nm (at 260 nm, it is one-tenth of that of quartz). Its efficiency at low wavelengths is believed to be enhanced by diffuse radiation transfer and internal reflectance (1).

Teflon is also a recommended material for use in trace metal studies where the hydrophobic surface is less likely to result in adsorptive losses and is readily purified of trace metal contaminants by acid washing. The latter feature makes Teflon bottles an attractive alternative to quartz tubes for the UV irradiation of natural water samples. This treatment is of value in trace metal speciation studies where irradiation at natural pH values releases organically bound metals (3). The application to aluminium speciation is of particular concern since the possibility of adsorptive losses of released aluminium, as both hydrolyzed and polymerized species, is high at natural pH values.

To examine this, samples of seawater and freshwater containing aluminium complexes were irradiated in both batch and continuous flow reactors. The former used Teflon FEP bottles (Nalgene Labware) of 60-mL capacity, in the 550-W irradiation rig described previously (4). Coil irradiations were carried out using an 8-ft length of Teflon FEP tubing ( $1/16$  in. o.d.  $\times$  0.012 in. i.d.) coiled around a Pen-Ray Model 3SC-9 UV lamp (Ultra-Violet Products Inc., CA) enclosed in an aluminium block. Solutions were pumped through the coil at variable flow rates. Teflon bottles and tubing were cleaned before use by soaking overnight in dilute nitric acid followed by rinsing with distilled water and sample.

Analysis of the batch irradiated samples showed more reactive aluminium in solution in samples contained in Teflon bottles than those in quartz. Closer examination revealed that this was due to a decrease in pH of the solutions in Teflon to 3.5 and soluble fluoride ion concentrations as high as 20 mg L<sup>-1</sup> (Table I), which apparently resulted from photode-

composition of the Teflon surface. The effect of irradiation time is shown in Table I. Fluoride release also occurred from acidified samples. The same containers are used for six subsequent runs with similar results being obtained.

The slow initial increase in fluoride ion with time suggested a reaction temperature effect. The temperature of the sample in the Teflon bottle reached 55 °C, although the outer surface of the bottle was significantly hotter, and this temperature would only be reached after irradiation for about 0.5-1 h. When placed in a water-jacketed quartz container, the sample in the bottle was kept at an ambient temperature of 30 °C although the incident radiation was reduced. Under these conditions the rate of formation of fluoride decreased significantly with 0.9 mg L<sup>-1</sup> being detected after a 4-h irradiation. Even so, this concentration is sufficient to complex aluminium at microgram per liter concentrations.

When the coil reactor was used, it was not possible to cool the lamp and the temperature on the outside of the Teflon tubing reached 48 °C, as specified by the manufacturer. When the solution flow rate was lowered, the contact time of the solution with the surface increased and raised the temperature of the solution. Fluoride release approximated a linear function of solution residence time in the coil. For flow rates of 0.5 and 1.0 mL min<sup>-1</sup>, respectively, effluent fluoride concentrations of 12 and 5 mg L<sup>-1</sup> were detected. For effective photodecomposition to occur, recommended flow rates for postcolumn photochemical reactors are between 0.5 and 1.0 mL min<sup>-1</sup> (2, 5).

The use of Teflon coils in photoconductivity detectors should therefore result in a high background conductance which would significantly limit the sensitivity of the detector. For example, for a 350-ng injection of 2,3,7,8-tetrachlorodioxin, assuming 1% photolysis as approximated by Popovich et al. (5) for a quartz reactor, the solution chloride ion concentration reaching the conductance cell would be in the range 10-20  $\mu$ g L<sup>-1</sup> compared to a background fluoride ion concentration of 5-10 mg L<sup>-1</sup>.

Workers contemplating the use of Teflon components in photochemical reactors are therefore cautioned to consider whether in their particular application fluoride and hydrogen